Table 30.1 Parameters of fibrogenesis and oxidative stress in serum and liver tissue

Parameter	tissue	(unit)	Normal group	LD group	LDT group
Hydroxyproline	liver	(μg/L)	16.10 ± 6.04	304.83 ± 128.77[a]	212.27 ± 81.49[ab]
TGF−β_1 mRNA	liver		0.03 ± 0.01	0.98 ± 0.25[a]	0.45 ± 0.25[ab]
LPO	serum	(μmol/L)	1.11 ± 0.68	12.40 ± 5.09[a]	3.04 ± 1.91[ab]
	liver	(μmol/L)	0.88 ± 0.59	31.70 ± 11.35[a]	14.86 ± 14.2[ab]
8-OHdG	serum	(μmol/L)	1.58 ± 0.55	15.27 ± 4.7[a]	11.71 ± 4.41[ab]
	liver	(ng/g)	1.76 ± 0.39	9.27 ± 2.48[a]	6.88 ± 0.95[ab]

TGF−β_1 mRNA is expressed relative to β-actin mRNA. a and b show significant difference ($P < 0.05$) compared to the normal and LD groups, respectively, by one-way ANOVA post hoc Fisher's PLSD test. Data represent means±SD.

significantly reduced, and the architecture of the hepatic parenchyma and lobules was preserved. The fibrotic area quantified from the positive silver staining was 21.6 ± 9.1% in the LD group and 8.0 ± 5.9% in the LDT group, although there was no significant difference between the groups. Based on Western blot analysis and IHC staining, the number and intensity of α-SMA of the LD group was markedly increased compared to those of the LDT group.

30.3.1.3 Fibrogenesis and Oxidative Stress Markers

Hepatic hydroxyproline content and TGF−β_1 mRNA levels of the LD and LDT groups were significantly increased compared to those of the normal group, with the levels being significantly lower in the LDT group than in the LD group (Table 30.1). Likewise, the LPO and 8-OHdG content of serum and liver was significantly increased in both the LD and LDT groups compared to that of the normal group, but content was significantly lower in the LDT group than in the LD group.

30.3.2 Primary HSC Cultured with Taurine

30.3.2.1 HSC Proliferation and Signaling Pathways of Cell Growth

Cell growth of HSC assessed by the MTT assay was significantly decreased in cells cultured with 50 mM taurine compared to those cultured without taurine (Fig. 30.3). There was also a significant difference between cells incubated with medium containing 25 mM taurine for 6 days (condition C) compared to those cultured without taurine. Similarly, based on the BrdU assay, DNA synthesis of the 50 mM taurine group was significantly reduced compared to that of the 0 mM taurine group. For conditions B and C, DNA synthesis was significantly lower in the 50 mM taurine group than in the 25 mM taurine group. HSC incubated with taurine according to condition A showed no significant difference in total and phosphorylated forms of the MAPKs and Akt.

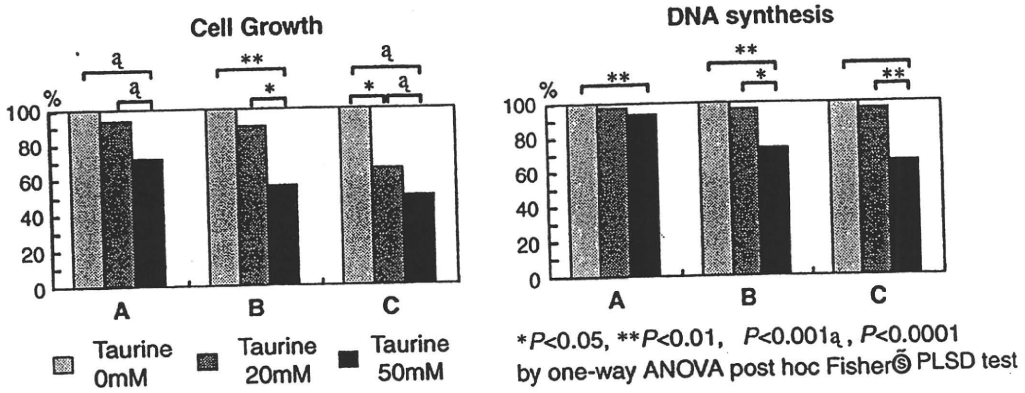

Fig. 30.3 Cell proliferation of primary cultured HSC treated with taurine. Cell growth and DNA synthesis were analyzed by MMT and BrdU assays. **Condition A:** cultured with taurine for 3 days, **Condition B:** cultured with taurine for 3 days followed by 3 days without taurine, **Condition C:** cultured with taurine for 6 days. Data represent means±SD

30.3.2.2 Fibrogenesis and Oxidative Stress Factors of Cultured HSC

When incubated according to condition A, TGF−β_1 mRNA content of TAU-25 (0.02 ± 0.01 fold compared to β-actin) and -50 (0.03 ± 0.01) was significantly decreased compared to that of Tau-0 (0.04 ± 0.03, $P < 0.05$). However, there was no significant difference between the Tau-25 and -50 groups. The LPO and hydroxyproline content of culture medium collected before (Pre) and after treatment with taurine for 3 days (condition A) was higher in the Tau-0 (0.48±0.07 g/L and 7.16±3.85 μ mol/L, respectively) than in the Pre group (0.04±0.01, $P < 0.01$ and 1.92 ± 0.39, $P < 0.05$, respectively). The hydroxyproline concentration (g/L) was significantly lower in the Tau-50 (0.38 ± 0.08, $P < 0.05$) than in the Tau-0 group. The LPO concentration (μ mol/L) in the Tau-25 (4.84 ± 2.53, $P < 0.05$) and -50 (3.13±2.50, $P < 0.01$) groups was significantly decreased compared to those of the Tau-0 group. There was no significant difference between the hydroxyproline and LPO concentrations of the Tau-25 and -50 groups.

30.4 Discussion

In the present study, taurine treatment prevented the decline in hepatic taurine content of the CCl_4 treated rat. Taurine treatment also protected the liver against oxidative stress-induced damage trigger by repetitive CCl_4 administration in rats. Particularly noteworthy was the reduction in hepatic fibrosis of the CCl_4-administered rats treated with taurine. Furthermore, in the cultured HSC study, taurine inhibited the transformation of HSC while reducing oxidative stress. These results showed that fibrosis was directly inhibited by taurine through attenuation of oxidative stress-mediated transformation of HSC to myofibroblast-like cells. However, the mechanism of taurine-mediated modulation of cell proliferation of HSC remains unclear, but does not appear to involve the signaling pathways of MAPKs and

Akt. Therefore, there must be some other mechanism that can mediate the effect of taurine on HSC proliferation. Furthermore, the mechanism underlying taurine-mediated protection against liver disease must involve multiple factors because taurine diminished diverse types of hepatic damage, including hepatocyte necrosis, fatty degeneration, infiltration of inflammatory cells and fibrosis. Therefore, taurine acts through multiple and complex mechanisms, including cell membrane stabilization, osmoregulation, detoxification, anti-apoptosis, modulation of bile acid conjugation/excretion, cholesterol excretion, anti-inflammation, anti-oxidation, inhibition of fibrogenesis and cytokine secretion, inhibition of HSC transformation and inhibition of cytokine/autocrine action. In conclusion, taurine supplementation should be considered as a therapy to lessen the severity of oxidative stress-induced hepatic injury and fibrosis.

Acknowledgments This study was supported by a research grant from Taisho Pharmaceutical Co., Ltd. Japan. This study has been previously published in part in the *Journal of Hepatology* in 2005.

References

Awapara J (1956) The taurine concentration of organs from fed and fasted rats. J Biol Chem 218(2):571-6.

Azuma J, Hamaguchi T, Ohta H, Takihara K, Awata N, Sawamura A, Harada H, Tanaka Y, Kishimoto S (1987) Calcium overload-induced myocardial damage caused by isoproterenol and by adriamycin: possible role of taurine in its prevention. Adv Exp Med Biol 217:167–179

Balkan J, Dogru-Abbasoglu S, Kanbagli O, Cevikbas U, Aykac-Toker G, Uysal M (2001) Taurine has a protective effect against thioacetamide-induced liver cirrhosis by decreasing oxidative stress. Hum Exp Toxicol 20:251–254

Danielsson H (1963) Present status of research on catabolism, excretion of cholesterol. Adv Lipid Res 1:335–385

Davison AN, Kaczmarec LK (1971) Taurine-a possible neurotransmitter? Nature 234:107–108

Dinçcer S, Özenirler S, Öz E, Akyol G, Özogul C (2002) The protective effect of taurine pretreatment on carbon tetrachloride-induced hepatic damage – A light and electron microscopic study. Amino Acids 22:417–426

Enzan H, Himeno H, Iwamura S, Saibara T, Onishi S, Yamamoto Y, Hara H (1994) Immunohistochemical identification of Ito cells and their myofibroblastic transformation in adult human liver. Virchows Arch 424:249–256

Friedman SL (1993)Seminars in medicine of the Beth Israel Hospital, Boston. The cellular basis of hepatic fibrosis. Mechanisms and treatment strategies. N Engl J Med 328:1828–1835

Fukuda K, Hirai Y, Yoshida H, Nakajima T, Usui T (1982) Free amino acid content of lymphocytes and granulocytes compared. Clin Chem 28:1758–1761

Gordon RE, Heller RF, Heller RF (1992) Taurine protection of lungs in hamster models of oxidant injury: a morphologic time study of paraquat and bleomycin treatment. Adv Exp Med Biol 315:319–328

Green TR, Fellman JH, Eicher AL, Pratt KL (1991) Antioxidant role and subcellular location of hypotaurine and taurine in human neutrophils. Biochim Biophys Acta 1073:91–97

Gressner AM (1996) Transdifferentiation of hepatic stellate cells (Ito cells) to myofibroblasts: a key event in hepatic fibrogenesis. Kidney Int Suppl 54:S39–S45

Hosokawa Y, Matsumoto A, Oka J, Itakura H, Yamaguchi K (1990) Isolation and characterization of a cDNA for rat liver cysteine dioxygenase. Biochem Biophys Res Commun 168:473–478

Huxtable RJ (1980) Does taurine have a function? Fed Proc 39:2678–2679
Huxtable RJ (1992) Physiological actions of taurine. Physiol Rev 72:101–163
Jacobsen JG, Swimth LH (1968) Biochemistry and physiology of taurine and taurine derivatives. Physiol Rev 48:424–511
Kaisaki PJ, Jerkins AA, Goodspeed DC, Steele RD (1995) Cloning and characterization of rat cysteine sulfinic acid decarboxylase. Biochim Biophys Acta 1262:79–82
Kanner BI, Nurit KD (1994) Structure and function of sodium-coupled neurotransmitter transporters. Cell Physiol Biochem 4:174
Koyama I, Nakamura T, Ogasawara M, Nemoto M, Yoshida T (1992) The protective effect of taurine on the biomembrane against damage produced by the oxygen radical. Adv Exp Med Biol 315:355–359
Kuriyama K (1980) Taurine as a neuromodulator. Fed Proc 39:2680–2684
Li D, Friedman SL (1999) Liver fibrogenesis and the role of hepatic stellate cells: new insights and prospects for therapy. J Gastroenterol Hepatol 14:618–633
Ludwig J (1993) The nomenclature of chronic active hepatitis:an obituary. Gastroenterol 105: 274–278
Matsuzaki Y, Miyazaki T, Miyakawa S, Bouscarel B, Ikegami T, Tanaka N (2002a) Decreased taurine concentration in skeletal muscles after exercise for various durations. Med Sci Sports Exerc 34:793–797
Matsuzaki Y, Miyazaki T, Ohkoshi N, Miyakawa S, Bouscarel B, Tanaka N (2002b) Degeneration of skeletal muscle fibers in the rat administrated carbon tetrachloride:similar histological findings of the muscle in a 64-year-old patient of LC with muscle cramp. Hepatol Res 24:368–378
Mihaljevic B, Katusin-Razem B, Razem D (1996) The reevaluation of the ferric thiocyanate assay for lipid hydroperoxides with special considerations of the mechanistic aspects of the response. Free Radic Biol Med 21:53–63
Miyazaki T, Ikegami T, Zhang Y, Honda A, Doy M, Matsuzaki Y (2005) The prevention mechanisms of taurine on hepatic damage and fibrosis via antioxidative stress. Jpn Pharmacol Ther 33:S105
Miyazaki T, Matsuzaki Y, Ikegami T, Miyakawa S, Doy M, Tanaka N, Bouscarel B (2004a) Optimal and effective oral dose of taurine to prolong exercise performance in rat. Amino Acids 27:291–298
Miyazaki T, Matsuzaki Y, Ikegami T, Miyakawa S, Doy M, Tanaka N, Bouscarel B (2004b) The harmful effect of exercise on reducing taurine concentration in the tissues of rats treated with CCl_4 administration. J Gastroenterol 39:557–562
Miyazaki T, Matsuzaki Y, Karube M, Bouscarel B, Miyakawa S, Tanaka N (2003a) Amino acid ratios in plasma and tissues in a rat model of liver cirrhosis before and after exercise. Hepatol Res 27:230–237
Miyazaki T, Matsuzaki Y, Karube M, Miyakawa S, Tanaka N (2003b) Clinical importance of taurine maintenance on liver disease. Gastroenterology 37:558–562
Nakashima T, Seto Y, Nakajima T, Shima T, Sakamoto Y, Cho N, Sano A, Iwai M, Kagawa K, Okanoue T, et al. (1990) Calcium-associated cytoprotective effect of taurine on the calcium and oxygen paradoxes in isolated rat hepatocytes. Liver 10:167–172
Nakatsukasa H, Nagy P, Evarts RP, Hsia CC, Marsden E, Thorgeirsson SS (1990) Cellular distribution of transforming growth factor-beta 1 and procollagen types I, III, and IV transcripts in carbon tetrachloride- induced rat liver fibrosis. J Clin Invest 85:1833–1843
Nieminen ML, Tuomisto L, Solatunturi E, Eriksson L, Paasonen MK (1988) Taurine in the osmoregulation of the Brattleboro rat. Life Sci 42:2137–2143
Pasantes MH, Wright CE, Gaull GE (1984) Protective effect of taurine, zinc and tocopherol on retinol-induced damage in human lymphoblastoid cells. J Nutr 114:2256–2261
Pasantes MH, Wright CE, Gaull GE (1985) Taurine protection of lymphoblastoid cells from iron-ascorbate induced damage. Biochem Pharmacol 34:2205–2207
Reymond I, Sergeant A, Tappaz M (1996) Molecular cloning and sequence analysis of the cDNA encoding rat liver cysteine sulfinate decarboxylase (CSD). Biochim Biophys Acta 1307: 152–156

Schafer S, Zerbe O, Gressner AM (1987) The synthesis of proteoglycans in fat-storing cells of rat liver. Hepatology 7:680–687

Sjovall J (1959) Dietary glycine and taurine on bile acid conjugation in man; bile acids and steroids 75. Proc Soc Exp Biol Med 100:676–678

Sturman JA (1993) Taurine in development. Physiol Rev 73:119–147

Tappaz M, Bitoun M, Reymond I, Sergeant A (1999) Characterization of the cDNA coding for rat brain cysteine sulfinate decarboxylase: brain and liver enzymes are identical proteins encoded by two distinct mRNAs. J Neurochem 73:903–912

Timbrell JA, Seabra V, Waterfield CJ (1995) The in vivo and in vitro protective properties of taurine. Gen Pharmacol 26:453–462

Vohra BP, Hui X (2001) Taurine protects against carbon tetrachloride toxicity in the cultured neurons and in vivo. Arch Physiol Biochem 109:90–94

Wang QJ, Giri SN, Hyde DM, Li C (1991) Amelioration of bleomycin-induced pulmonary fibrosis in hamsters by combined treatment with taurine and niacin. Biochem Pharmacol 42:1115–1122

Waterfield C.J, Mesquita M, Parnham P, Timbrell J.A (1993a) Taurine protects against the cytotoxicity of hydrazine, 1,4-naphthoquinone and carbon tetrachloride in isolated rat hepatocytes. Biochem Pharmacol 46:589–595

Waterfield CJ, Turton JA, Scales MD, Timbrell JA (1993b) Reduction of liver taurine in rats by beta-alanine treatment increases carbon tetrachloride toxicity. Toxicology 29:7–20

Wright CE, Lin TT, Lin YY, Sturman JA, Gaull GE (1985) Taurine scavenges oxidized chlorine in biological systems. Prog Clin Biol Res 179:137–147

Zhang Y, Ikegami T, Honda A, Miyazaki T, Bouscarel B, Rojkind M, Hyodo I, Matsuzaki Y (2006) Involvement of integrin-linked kinase in carbon tetrachloride-induced hepatic fibrosis in rats. Hepatology 44:612–622

70 (140) 2009 Vol.54 No.2

自己免疫性肝疾患類似GVHRマウスモデルの肝病変に対する制御性T細胞の関与

東京医科大学地域医療振興学寄付講座[1],
東京医科大学茨城医療センター共同研究センター[2],
茨城県立中央病院[3], 東京医科大学茨城医療センター消化器内科[4],
霞ヶ浦成人病研究事業団[5]
宮﨑 照雄[1,2], 土井 幹雄[3], 伊藤 進一[4,5], 本多 彰[1,2]
池上 正[4], 松﨑 靖司[1,4]

はじめに

われわれはこれまで，肝特異的マウス移植片対宿主反応(GVHR)モデルを作製し，自己免疫性肝疾患の病態解析を行ってきた[1-4]。GVHRモデルは，C57BL/6(B6)雄マウスとMHC class IIの3つのアミノ酸の異なるB6.C-H-$2^{bm/2}$雌マウスを交配して得られたF1雌マウスに，B6雌マウスの脾臓より分離した1×10^7個のT細胞を尾静脈へ注射することで作製される(**図1**)。その結果，胆管上皮細胞に異所性にMHC class IIの発現がみられ，自己免疫機序が関与した門脈域，中心静脈周囲にrecipients由来のリンパ球を中心とした炎症性細胞浸潤が認められる。また，自己抗体(抗核抗体，抗ミトコンドリア抗体)の産生が確認される。肝組織への炎症性細胞浸潤は，GVHR導入後5目より確認され，その後，2週目でピークを迎える。しかし，GVHR導入2週目以降，自然経過観察下で炎症性細胞浸潤面積，浸潤部位数共に有意に減少し，線維化や肝硬変には至らず改善してしまう。このモデル特有のGVHR導入後一過性の炎症からの改善のメカニズムを明らかにすることは，自己免疫性肝疾患の病態解明への一助になると考えられる。

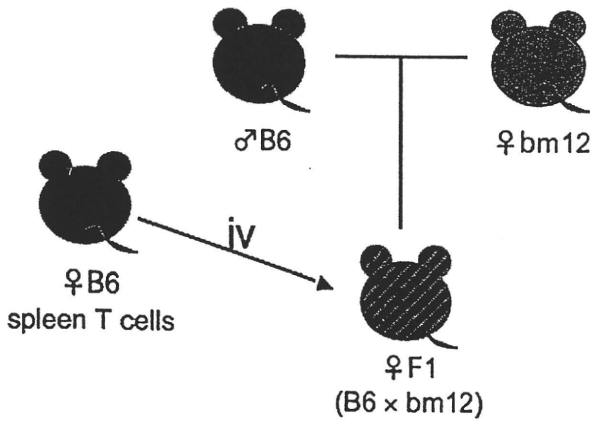

図1 マウスGVHRモデル

今研究では，このGVHRモデル肝病変改善の原因を明らかにする目的で，肝組織内の免疫寛容獲得過程に関与する遺伝子群について，網羅的遺伝子発現頻度解析とその結果に基づいて浸潤内炎症性細胞群に対して免疫組織的解析を行った。

方 法

GVHR導入直後，2，4，8週目(G0，G2，G4，G8)のマウスより肝組織を採取した。遺伝子解析には，G0，G2，G8を用い，同週令の正常マウスをコントロールとし，炎症性サイトカイン関連遺伝子514種についてシグマ社のPanorama® Mouse Cytokine Gene Arrayを用いた。whole liverからtotal RNAを抽出し，逆転写の際にcDNAに[α-^{33}P]dCTPをラベル化させ，そのcDNAをgene arrayにhybridizationさせた。spotの強度は，normalization後，2倍以上の強度を増加，1/2倍以上を減少とした。

組織学的解析は，G0，G2，G4，G8から採取した肝組織からパラフィン切片を作製し，HE染

色と浸潤リンパ球に対しCD4，CD8，CD20，CD25，CD45ro，CD161，IL-10レセプター[R]β，FoxP3の免疫染色を行い，各陽性細胞数の定量を行った。また，制御性T(Treg)細胞表面マーカー(CD4，CD25，CD161，IL-10Rβ)において，蛍光二重免疫染色を行った。

更に，免疫組織学解析の結果を検証するため，F1マウスに抗IL-10抗体もしくはモノクローナル抗体(Rat IgG Isotype)を腹腔内に投与し，その4時間後，GVHR導入を行い，その後2週目の肝病態変化を観察した(図2)。

結　果

Gene arrayの解析の結果，514遺伝子の変化は3パターンに分類された。G0からG8まで変化がないパターンに，448遺伝子が該当した。それ以外は，G0に比しG2で増加し，その後，G8で減少するパターンの20遺伝子と，G8まで維持するパターンの46遺伝子であった。ちなみに，G0からG2で減少，G2からG8で増加するパターンはなかった。病態改善と共に変動するパターンの20遺伝子のうち，G2時点で最も発現が高い遺伝子は，IL-2Rγであった。この結果から，IL-2Rの一部を共に構成するIL-2Rα(CD25)との関わりあいを推測し，近年，自己免疫疾患などの免疫寛容破綻への免疫制御が注目されているTreg細胞(CD4$^+$CD25$^+$T細胞，CD161$^+$NKT細胞，IL-10R$^+$Tr1細胞など)に着目するに至った。

免疫染色の結果，肝組織内浸潤炎症性細胞群にTreg細胞マーカー(CD25，FoxP3，IL-10R，CD161)を含め，今研究で検討した表面マーカーすべてにおいて，陽性細胞が認められた(図3)。

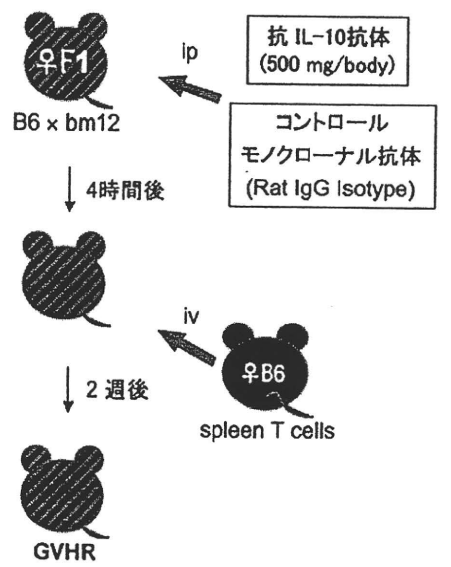

図2　抗IL-10抗体投与GVHRマウス

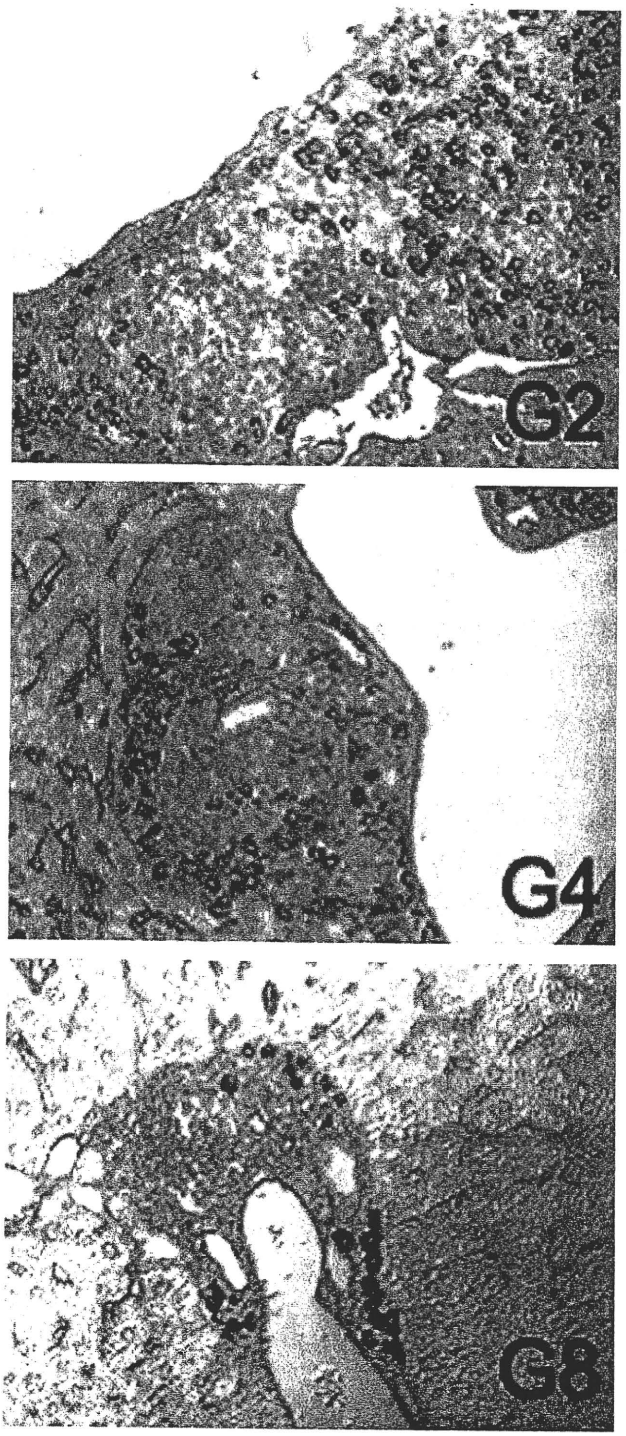

図3　肝組織内浸潤CD4陽性細胞免疫染色像

更に，蛍光二重染色の結果，Treg 細胞マーカーは，それぞれ CD4 との共発現がみられ，免疫染色による陽性細胞が Treg 細胞であることを確認した。

G2，G4，G8 における各マーカー陽性細胞数は，肝病態改善と共に G2 から G8 にかけ有意に減少した。しかし，IL-10R$^+$ 細胞のみ，G8 までの発現量が維持していた。

そこで，GVHR の病態改善に対する Tr1 細胞発現の意義を抗 IL-10 抗体投与 GVHR マウスにおいて確認した。抗 IL-10 抗体投与により，GVHR マウスの肝組織内炎症性細胞浸潤域に IL-10R$^+$ 細胞浸潤は完全に抑制された。それに伴い，モノクローナル抗体投与 GVHR マウスと比較して，炎症性細胞浸潤が有意に増悪した。また，抗 IL-10 抗体投与 GVHR マウス肝組織内において，FoxP3$^+$ 細胞の有意な浸潤増加が観察された。

考察・結論

遺伝子解析ならびに免疫組織化学染色の結果，GVHR モデル肝組織内に Treg 細胞の出現が認められ，病態改善過程において Tr1 細胞の発現が持続していた。このことから，GVHR 導入後，自己免疫寛容の破綻が生じ，肝に炎症性細胞浸潤が生じるが，この Tr1 細胞が関与することで自己免疫寛容が再獲得され，病態が一過性のものとして生じている可能性が示唆された(図 4)。これは，抗 IL-10 抗体投与 GVHR マウスで，Tr1 細胞の肝内浸潤領域内での発現を抑制させたところ，炎症性細胞浸潤が増悪したことから，病態改善への Tr1 細胞の関与を大きく支持するものと考えられる。また，IL-10 抗体投与 GVHR マウスで，FoxP3$^+$ 細胞の浸潤が有意に増加したのは，発現抑制された Tr1 細胞の末梢組織での分化を促進するためのフィードバックによるものと推測される[5,6]。

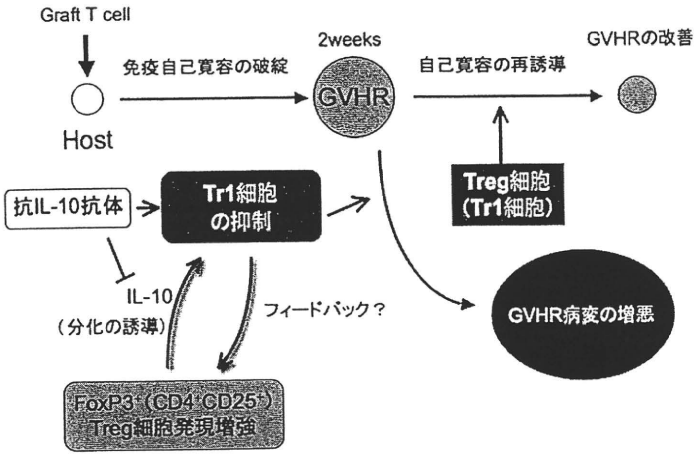

図 4　GVHR モデルにおける Treg 細胞の免疫寛容制御機序

文　献

1) Itoh S, Matsuzaki Y, Kimura T, *et al.*: Cytokine profile of liver-infiltrating CD4$^+$ T cells separated from murine primary biliary cirrhosis-like hepatic lesions induced by graft-versus-host reaction. J Gastroenterol Hepatol 2000; **15**: 443-451.
2) Itoh S, Matsuzaki Y, Kimura T, *et al.*: Suppression of hepatic lesions in a murine graft-versus-host reaction by antibodies against adhesion molecules. J Hepatol 2000; **32**: 587-595.
3) Unno R, Matsuzaki Y, Itoh S, *et al.*: Novel murine autoimmune-mediated liver disease model induced by graft-versus-host reaction and concanavalin A. J Gastroenterol Hepatol 2001; **16**: 1149-1157.
4) Unno R, Matsuzaki Y, Itoh S, *et al.*: Progression of autoimmune-mediated hepatic lesions in a murine graft-versus-host reaction by neutralizing IL-10. Hepatol Res 2003; **26**: 354-361.
5) Thompson C, Powrie F: Regulatory T cells. Curr Opin Pharmacol 2004; **4**: 408-414.
6) Veldman C, Nagel A, Hertl M: Type I regulatory T cells in autoimmunity and inflammatory diseases. Int Arch Allergy Immunol 2006; **140**: 174-183.

Highly sensitive quantification of serum malonate, a possible marker for de novo lipogenesis, by LC-ESI-MS/MS

Akira Honda,*,† Kouwa Yamashita,§ Tadashi Ikegami, Takashi Hara,†† Teruo Miyazaki,*,† Takeshi Hirayama,** Mitsuteru Numazawa,§ and Yasushi Matsuzaki[1,†,**]**

Center for Collaborative Research,* Department of Development for Community Medicine,† and Department of Gastroenterology,** Tokyo Medical University Ibaraki Medical Center, Ami, Ibaraki 300-0395, Japan; Faculty of Pharmaceutical Science,§ Tohoku Pharmaceutical University, Sendai, Miyagi 981-8558, Japan; and Ibaraki Prefectural Institute of Public Health,†† Mito, Ibaraki 310-0852, Japan

Abstract We describe a new sensitive and specific method for the quantification of serum malonate (malonic acid, MA), which could be a new biomarker for de novo lipogenesis (fatty acid synthesis). This method is based upon a stable isotope-dilution technique using LC-MS/MS. MA from 50 μl of serum was derivatized into di-(1-methyl-3-piperidinyl)malonate (DMP-MA) and quantified by LC-MS/MS using the positive electrospray ionization mode. The detection limit of the DMP-MA was approximately 4.8 fmol (500 fg) (signal-to-noise ratio = 10), which was more than 100 times more sensitive compared with that of MA by LC-MS/MS using the negative electrospray ionization mode. The relative standard deviations between sample preparations and measurements made using the present method were 4.4% and 3.2%, respectively, by one-way ANOVA. Recovery experiments were performed using 50 μl aliquots of normal human serum spiked with 9.6 pmol (1 ng) to 28.8 pmol (3 ng) of MA and were validated by orthogonal regression analysis. The results showed that the estimated amount within a 95% confidence limit was 14.1 ± 1.1 pmol, which was in complete agreement with the observed $\bar{X}_0$ = 15.0 ± 0.6 pmol, with a mean recovery of 96.0%. This method provides reliable and reproducible results for the quantification of MA in human serum.—Honda, A., K. Yamashita, T. Ikegami, T. Hara, T. Miyazaki, T. Hirayama, M. Numazawa, and Y. Matsuzaki. **Highly sensitive quantification of serum malonate, a possible marker for de novo lipogenesis, by LC-ESI-MS/MS.** *J. Lipid Res.* **2009.** 50: **2124–2130.**

Supplementary key words acetyl-CoA carboxylase • carnitine palmitoyl transferase 1 • fatty acid synthase • liquid chromatography-electrospray ionization-tandem mass spectrometry • malonic acid • malonyl-CoA • malonyl-CoA decarboxylase

Acetyl-CoA carboxylase (ACC) is the rate-controlling enzyme in the fatty acid biosynthetic pathway, and catalyzes the formation of malonyl-CoA from acetyl-CoA plus bicarbonate. Malonyl-CoA is not only substrate for fatty acid synthase (FAS) but is also a potent inhibitor of carnitine palmitoyl transferase 1 (1), the rate-limiting enzyme of fatty acid β-oxidation. Therefore, malonyl-CoA is a key molecule that controls fatty acid metabolism in the body. In addition, recent studies have shown that the level of hypothalamic malonyl-CoA is dynamically regulated by fasting and feeding and that it alters subsequent feeding behavior (2).

To determine ACC activity in tissues, an invasive tissue biopsy is necessary. However, whole body synthesis of fatty acid may be evaluated by the quantification of serum malonyl-CoA metabolites. This concept originates from our previous studies, which showed that serum concentrations of the immediate products of the rate-controlling enzymes in cholesterol and bile acid biosynthetic pathways reflected the activities of the rate-controlling enzymes and whole body cholesterol and bile acid biosynthesis (3). Furthermore, patients with malonyl-CoA decarboxylase (MCD) deficiency, who must have increased tissue malonyl-CoA concentrations, are characterized by markedly elevated urinary malonic acid (MA), called "malonic aciduria" (4). This phenomenon suggests that malonyl-CoA is easily hydrolyzed into MA by an unidentified tissue thioesterase(s). Therefore, we thought that serum MA concentrations might well reflect total body FAS.

This work was supported in part by a Grant-in-Aid for Scientific Research (C20591309) from the Japan Society for the Promotion of Science and a grant from the Ministry of Education, Culture, Sports, Science and Technology of Japan.

Manuscript received 1 December 2008 and in revised form 15 April 2009.

Published, JLR Papers in Press, April 29, 2009
DOI 10.1194/jlr.D800054-JLR200

Abbreviations: ACC, acetyl-CoA carboxylase; DMP-MA, Di-(1-methyl-3-piperidinyl)malonate; FAS, fatty acid synthase; MA, malonic acid (malonate); MCD, malonyl-CoA decarboxylase; MMA, methylmalonic acid (methylmalonate); N-ESI, ESI in negative mode; P-ESI, ESI in positive mode; SA, succinic acid (succinate); SRM, selected reaction monitoring.

[1]To whom correspondence should be addressed.
e-mail: ymatsuzaki-gi@umin.ac.jp

Although methodological reports for the quantification of serum MA are not available, there have been some reports that describe the methods for the determination of urinary MA levels in patients with MCD deficiency by gas chromatography (5, 6) or gas chromatography-mass spectrometry (7). In these methods, urinary organic acids were extracted with ethyl acetate and converted into trimethylsilyl derivatives before analysis. Alternatively, blood malonylcarnitine has been measured for the diagnosis of MCD deficiency using liquid chromatography-tandem mass spectrometry coupled with electrospray ionization mode (LC-ESI-MS/MS) (8). However, because all of these methods were developed to diagnose markedly elevated MA levels in patients with MCD deficiency, the authors did not pay significant attention to the sensitivities of the methods.

The aim of this study was to measure serum MA concentrations in normal human subjects with sufficient sensitivity and specificity. For this purpose, serum MA was derivatized into di-(1-methyl-3-piperidinyl)malonate (DMP-MA) and quantified using positive LC-ESI-MS/MS (LC-P-ESI-MS/MS).

MATERIALS AND METHODS

Chemicals

MA and [$^{13}C_3$]MA were purchased from Sigma-Aldrich Chemical Co. (St. Louis, MO). 3-Hydroxy-1-methylpiperidine and 2-methyl-6-nitrobenzoic anhydride were purchased from Tokyo Kasei Kogyo (Tokyo, Japan) and 4-dimethylaminopyridine and formic acid were obtained from Wako Pure Chemical Industries (Osaka, Japan). Additional reagents and solvents were of analytical grade.

Sample collection

Blood samples were collected from healthy human volunteers. After coagulation and centrifugation at 1,500 *g* for 10 min, serum samples were stored at −20°C until analysis. Informed consent was obtained from all subjects, and the experimental procedures were conducted in accordance with the ethical standards of the Helsinki Declaration. Rat serum was prepared in our previous study (9) and had been stored at −20°C until it was used in the present experiments.

Sample preparation

Fifty μl of serum was placed in a microcentrifuge tube (1.5 ml, Eppendorf, Hamburg, Germany), and 19.2 pmol (2 ng) of [$^{13}C_3$] MA in 100 μl of acetonitrile as an internal standard. The sample tube was vortexed for 1 min and centrifuged at 2,000 *g* for 1 min. The solution of internal standard in acetonitrile led to deproteinization of the sample and the liquid phase was collected and evaporated to dryness at 80°C under a nitrogen stream. Derivatization of MA into DMP-MA was performed according to the Shiina method for the synthesis of carboxylic esters (10) with some modifications. The reagent mixture for derivatization consisted of 2-methyl-6-nitrobenzoic anhydride (67 mg), 4-dimethylaminopyridine (20 mg), pyridine (900 μl), and 3-hydroxy-1-methylpiperidine (100 μl). The freshly prepared reagent mixture (100 μl) was added to the serum extract and the reaction mixture was allowed to stand at room temperature for 30 min. After the addition of 2 ml of n-hexane, the mixture was vortexed for 30 s and centrifuged at 700 *g* for 2 min. The clear supernatant was collected and evaporated at 80°C under nitrogen. The residue was redissolved in 50 μl of 1% formic acid in water and an aliquot (1 μl) was injected into the following LC-MS/MS system.

Determination of DMP-MA by LC-P-ESI-MS/MS

The LC-MS/MS system consisted of a TSQ Quantum Ultra quadrupole mass spectrometer (Thermo Fisher Scientific, San Jose, CA) equipped with an H-ESI probe and a Nanospace SI-2 HPLC system (Shiseido, Tokyo, Japan). Chromatographic separation was performed using a Hypersil GOLD aQ column (150 × 2.1 mm, 3 μm, Thermo Fisher Scientific) at 40°C. Initially, the mobile phase was comprised of 0.2% formic acid in water and was used at a flow rate of 200 μl/min for 5 min, and it was then switched to 0.2% formic acid in acetonitrile at a flow rate of 300 μl/min for an additional 3.5 min. The general LC-MS/MS conditions were as follows: spray voltage, 1000 V; vaporizer temperature, 350°C; sheath gas (nitrogen) pressure, 50 psi; auxiliary gas (nitrogen) flow, 40 arbitrary units; ion transfer capillary temperature, 350°C; collision gas (argon) pressure, 1.5 mTorr; collision energy, 15 V; and ion polarity, positive.

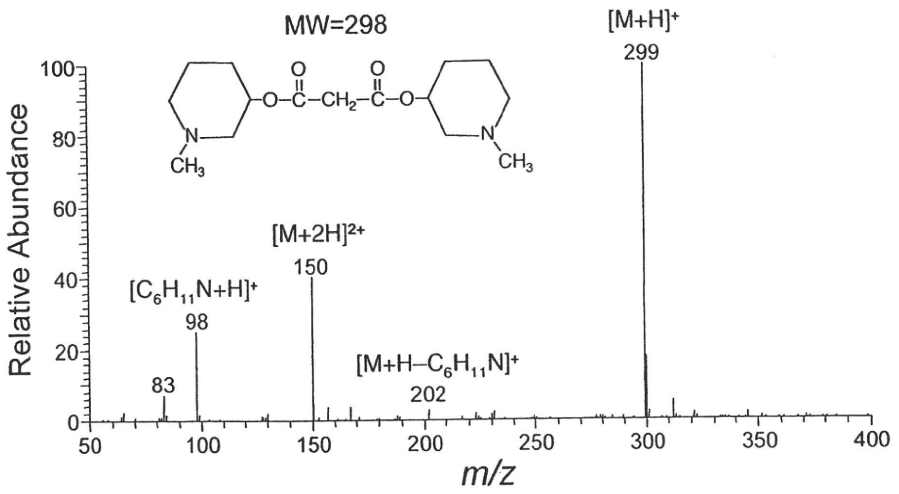

Fig. 1. Typical P-ESI mass spectrum of the DMP-MA. The general LC-MS/MS conditions were as described in Materials and Methods.

Determination of MA by LC-N-ESI-MS/MS

LC-negative (N)-ESI-MS/MS analysis of MA was carried out using the same LC-MS/MS instrument described above. Hypersil GOLD column (150 × 2.1 mm, 3 μm, Thermo Fisher Scientific) was used at 40°C. The mobile phase consisted of methanol-water (5:95, v/v) containing 0.2% formic acid and was used at a flow rate of 200 μl/min. The general LC-MS/MS conditions were as follows: spray voltage, 4000 V; vaporizer temperature, 350°C; sheath gas (nitrogen) pressure, 50 psi; auxiliary gas (nitrogen) flow, 30 arbitrary units; ion transfer capillary temperature, 300°C; collision gas (argon) pressure, 1.5 mTorr; collision energy, 15 V; and ion polarity, negative.

Statistics

Data are reported as the mean ± SD. Linearity of the calibration curve was analyzed by simple linear regression. Reproducibility was analyzed by one-way ANOVA (JMP software, SAS Institute, Inc., Cary, NC). The estimated amount ± 95% confidence limit was obtained as an index of precision (11). To calculate the values, orthogonal regression analysis was performed in the recovery study by using JMP software. For all analyses, significance was accepted at the level of $P < 0.05$.

RESULTS

Selected reaction monitoring

A typical ESI positive mass spectrum of the DMP-MA is shown in **Fig. 1**. This DMP ester derivative exhibited $[M+H]^+$ ion at *m/z* 299 as the base peak. In the MS/MS spectrum using *m/z* 299 as a precursor ion, the $[C_6H_{11}N+H]^+$ ion was observed at *m/z* 98 as the most prominent peak. The selected reaction monitoring (SRM) was conducted using *m/z* 299 → *m/z* 98 for the DMP-MA and *m/z* 302 → *m/z* 98 for the $[^{13}C_3]$ variant. We also monitored *m/z* 299 → *m/z* 202, a product ion containing the MA molecule

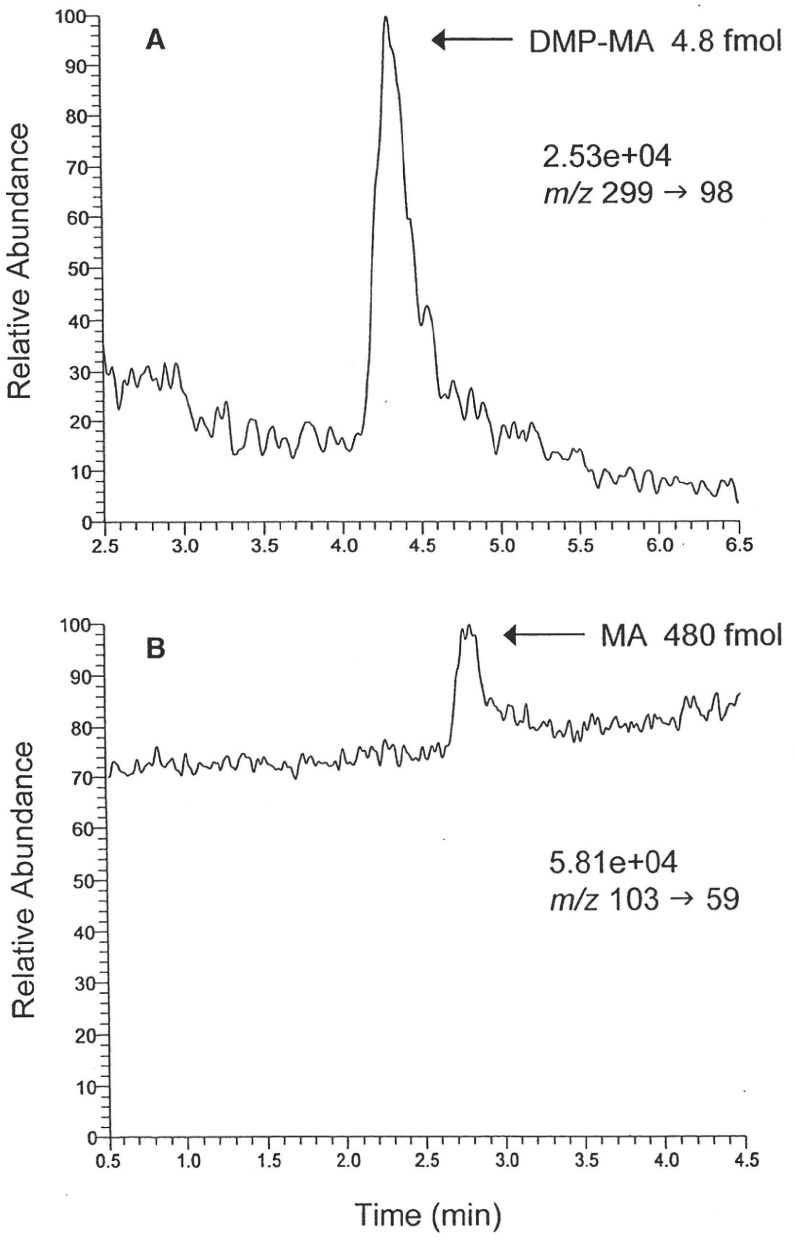

Fig. 2. Comparison of the detection limit of DMP-MA by LC-P-ESI-MS/MS at *m/z* 299 → *m/z* 98 (A) with that of MA by LC-N-ESI-MS/MS at *m/z* 103 → *m/z* 59 (B). Authentic standard of DMP-MA (4.8 fmol) or MA (480 fmol) was injected into the HPLC. The numbers written above the SRM ion pair represent the full scale of the chromatogram.

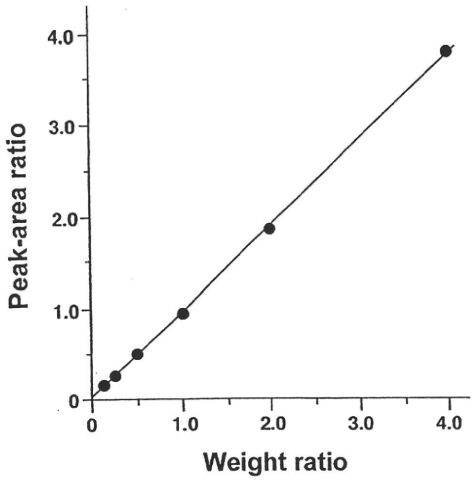

Fig. 3. Calibration curve for the weight ratio of MA to the corresponding deuterated internal standard. Linearity was checked by simple linear regression and the equation for the line of best fit was $y = 0.948x + 0.021$ (n = 6; $r = 1.000$; $P < 0.0001$).

but the former showed much better signal-to-noise ratio than the latter.

By N-ESI mode, authentic MA exhibited $[M-H]^-$ ion at *m/z* 103 as the base peak. In the MS/MS spectrum, the CH_3COO^- ion was observed at *m/z* 59 as the most prominent peak. The SRM was conducted using *m/z* 103 → *m/z* 59 for the MA.

Comparison of the sensitivities between P-ESI and N-ESI methods

To compare the sensitivity of DMP-MA by LC-P-ESI-MS/MS with that of MA by LC-N-ESI-MS/MS, the standard DMP-MA or MA solution was diluted and injected into the LC-MS/MS system. As shown in **Fig. 2A**, the DMP-MA was easily detected to 4.8 fmol by LC-P-ESI-MS/MS, with a signal-to-noise ratio of 10, whereas the conventional LC-N-ESI-MS/MS was barely able to detect 480 fmol of MA (Fig. 2B).

Calibration curve

A calibration curve was established for MA (**Fig. 3**). Each of different amounts (2.4, 4.8, 9.6, 19.2, 38.5, and 76.9 pmol) of authentic MA was mixed with 19.2 pmol of $[^{13}C_3]$MA, derivatized to the DMP ester and quantified as described in the Materials and Methods. The weight ratio of MA, relative to the corresponding ^{13}C-labeled internal standard, was plotted on the abscissa and the peak-area ratio of the DMP-MA to the $[^{13}C_3]$ variant measured by LC-P-ESI-MS/MS was plotted on the ordinate. The linearity of the standard curve, as determined by simple linear regression, was excellent for weight ratios between 0.125 and 4.0 (n = 6; $r = 1.000$; $P < 0.0001$).

Representative SRM

Figure 4 shows typical SRM chromatograms for DMP-MA and the $[^{13}C_3]$ variant obtained with 50 μl sera from a normal human (A) and a control rat (B). The peak-area ratio of the DMP-MA to the $[^{13}C_3]$ variant was calculated from the chromatograms, and MA amount was determined by applying the ratio to the calibration curve. The peaks of DMP-MA in chromatograms A and B correspond to ~0.66 pmol (0.66 μM) and ~4.43 pmol (4.43 μM), respectively.

Precision and accuracy of the LC-P-ESI-MS/MS method

The following studies were performed to determine the precision and accuracy of the present method using the same serum obtained from a normal human subject. Reproducibility was investigated by analyzing four samples in triplicate by LC-P-ESI-MS/MS (**Table 1**). The results were analyzed by a one-way ANOVA in which the analytical errors were divided into two sources, sample preparation

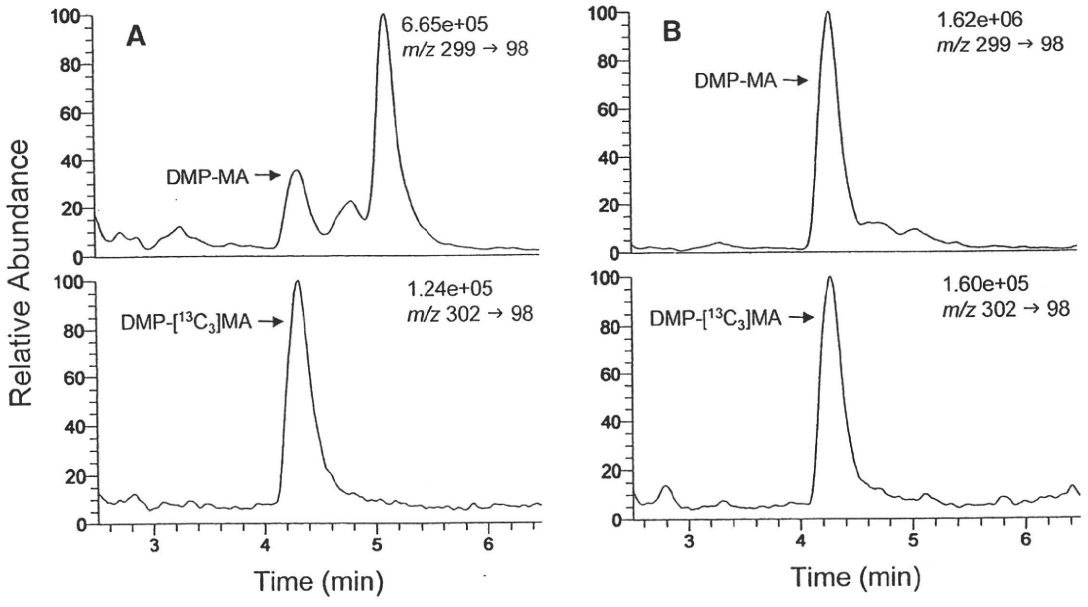

Fig. 4. Representative SRM chromatograms of DMP-MA and its $^{13}C_3$ variant (internal standard) obtained from 50 μl sera of a normal human (A) and a rat (B). The peaks of DMP-MA in chromatograms A and B correspond to ~0.66 pmol (0.66 μM) and ~4.43 pmol (4.43 μM), respectively. The numbers written above the SRM ion pair represent the full scale of the chromatogram.

TABLE 1. Reproducibility in the quantification of MA in human serum: analytical data

Sample	Individual Values			Mean ± SD
		pmol		
A	15.0	15.7	15.0	15.2 ± 0.38
B	14.4	15.6	15.5	15.2 ± 0.67
C	14.7	14.4	14.2	14.5 ± 0.29
D	15.6	15.6	14.7	15.3 ± 0.48
Mean ± SD				15.0 ± 0.58

MA was quantified in 50 μl of normal human serum.

and SRM measurement. The variances were not considered to be attributable to the sample preparation because the errors during sample preparation were not significantly larger than those between the measurements (**Table 2**). The inter-assay coefficients of variation for the between- and within-sample variations were 4.4% and 3.2%, respectively.

For the recovery experiments, known amounts of MA (a, 2a, 3a; a = 9.6 pmol) were spiked into 50 μl aliquots of the serum samples (n = 2). After the clean-up and derivatization procedures, SRM was carried out in triplicate for each sample. The recoveries of the known spiked amounts of MA ranged from 94.5% to 99.0%, with a mean of 96.0% (**Table 3**). In addition, the amount of endogenous MA found in unspiked 50 μl serum aliquots was within the 95% confidence limit for the estimated amount of MA calculated by orthogonal regression analysis, which also constituted an index for the precision and accuracy of the present method.

The circadian rhythm of MA levels in human sera

Figure 5 depicts the circadian rhythm of the serum concentrations of MA in a healthy male. Postprandial increases of MA concentrations (maximum 235% after dinner) were observed and the levels peaked between 2.5 and 6.5 h postmeal. The increase of MA concentration disappeared after skipping breakfast on the second day, which supports the idea that the diurnal pattern of serum MA concentrations is controlled mainly by food intake.

DISCUSSION

We describe a sensitive new LC-P-ESI-MS/MS method for the quantification of MA in serum. LC-N-ESI-MS/MS may be more suitable for the determination of negatively charged compounds, such as organic acids because the method does not require a derivatization step. However, as shown in Fig. 2, the sensitivity of N-ESI was not sufficient to quantify MA concentrations in a small volume of normal human serum.

Recently, we derivatized another organic acid, mevalonate, into mevalonyl-(2-pyrrolidin-1-yl-ethyl)-amide and measured it using LC-P-ESI-MS/MS (12). In this method, mevalonate was lactonized into mevalonolactone and then a tertiary amine moiety was introduced by a characteristic amidation reaction with a primary alkylamine. As a result, the tertiary amine moiety markedly promoted protonation and attomole levels of mevalonate were detected. In the present study, tertiary amine moieties were successfully introduced to MA by esterification with 3-hydroxy-1-methylpiperidine. Thus, the reaction for the synthesis of carboxylic esters by Shiina et al. (10) appears to be useful not only for the derivatization of alcohols (13) but also for that of carboxylic acids. This derivative, DMP-MA, exhibited $[M+H]^+$ as the base peak by P-ESI-MS and the detection limit by SRM was more than 100 times lower than that of underivatized MA by SRM with N-ESI mode.

The derivatization and purification steps in this method are very simple but it should be mentioned that there are two pitfalls to obtaining reliable and reproducible results. First, use of the anion exchange column cartridge gave unexpectedly high values of MA concentrations. Serum MA was extracted by this cartridge and interfering peaks on SRM chromatograms were markedly reduced by the addition of this purification step. However, the recoveries of known amounts of MA from this cartridge were always more than 100%, and additional experiments suggested that a significant amount of MA was produced from unknown substance(s) in organic solvents by this anion exchange column (data not shown). Plasma methylmalonic acid (MMA) and its isomer succinic acid (SA) are also known to be extracted by this column (14). We have derivatized MMA and SA into DMP-MMA and DMP-SA, respectively, and analyzed them by the same HPLC condition as that for DMP-MA. The SRM was conducted using *m/z* 313 → *m/z* 98 for both DMP-MMA and DMP-SA. The results showed that DMP-MMA and DMP-SA were much more hydrophobic than DMP-MA and both compounds were eluted during washout phase with 0.2% formic acid in acetonitrile (after 6 min).

Second, pH of the final sample solution should not be more than 7 because an alkaline condition easily hydrolyzes DMP-MA. After the derivatization step, most of the excess reagents and hydrophilic impurities were

TABLE 2. Reproducibility in the quantification of MA in human serum: ANOVA

Source	S	f	V	F_0	Relative SD
					%
Sample preparation	1.293	3	0.431	1.89	4.4
Error (SRM)	1.820	8	0.228		3.2
Total	3.113	11			
			$F(3,8,0.05)=4.07$		

S, residual sum of squares; f, number of degrees of freedom; f_1, $f_{\text{sample preparation}}$; f_2, f_{error}; V, unbiased variance; F_0, observed value following F distribution variance ratio ($V_{\text{sample preparation}}/V_{\text{error}}$); $F(f_1, f_2, \alpha)$, density function of F distribution with f_1 and f_2 degrees of freedom.

TABLE 3. Recovery of MA from human serum

Sample (X_0 + na) (n = 0,1,2,3)	Amount Added	Amount Found			Recovery[b] (Mean ± SD)	Estimated Amount ± 95% Confidence Limit[c]
	pmol				%	*pmol*
X_0	0	$\bar{X}_0 \pm$ SD = 15.0 ± 0.6[a]				14.1 ± 1.1
X_0 + a	9.6	23.6	25.2	25.0		
X_0 + a	9.6	24.2	23.6	23.3	94.5 ± 8.2	
X_0 + 2a	19.2	33.2	32.1	32.0		
X_0 + 2a	19.2	33.9	34.1	34.0	94.6 ± 5.1	
X_0 + 3a	28.8	43.8	43.9	43.0		
X_0 + 3a	28.8	44.1	43.6	43.2	99.0 ± 1.5	

Known amounts of MA were spiked into 50 μl of normal human serum before sample preparation.
[a] The value was obtained from Table 1.
[b] Recovery (%) = (amount found – $\bar{X}_0$) / amount added × 100.
[c] The estimated amount was calculated by orthogonal regression.

precipitated by the addition of n-hexane but significant amounts of 3-hydroxy-1-methylpiperidine and 4-dimethylaminopyridine were recovered with DMP-MA in the final residue of the extract. Therefore, it was necessary to dissolve the final residue in 1% formic acid in water to keep the pH of the solution less than 7. The mobile phase of the HPLC (0.2% formic acid in water) was not sufficient to neutralize the final extract.

The highly sensitive quantification of serum MA can be useful for monitoring of de novo FAS, also called de novo lipogenesis, in normal humans. The diurnal variation of serum MA levels in a healthy human (Fig. 5) was similar to the variation of de novo FAS determined in humans by continuous intravenous infusion of sodium [1-^{13}C]acetate and mass isotopomer distribution analysis (15, 16). According to Timlin et al. (16), de novo FAS peaked 4.2 h after ingestion of a meal whereas lipoprotein-triacylglycerol concentrations peaked at 2.0 h postmeal. Another study, by Hudgins et al. (15), showed that the maximum values of de novo FAS occurred in the evening, 3.0–9.0 h after the last meal, although the peak after every meal was not detected because a limited number of postprandial data points were obtained. In our data, postprandial increases of MA concentrations peaked between 2.5 h and 6.5 h after meals and the maximum value was observed in the night 6.0 h after dinner. In addition, the increase of MA concentration disappeared after skipping the meal. Thus, serum MA concentrations are regulated by food intake and appear to be a good marker that reflects de novo FAS in normal humans.

Because serum MA concentrations correlate well with de novo FAS, the most important enzyme that determines serum MA concentration is thought to be ACC, the rate-limiting enzyme in the fatty acid biosynthesis. In mammals, two ACC isoforms exist. Cytosolic ACC1 synthesizes malonyl-CoA, which participates in both de novo FAS and negative regulation of β-oxidation. In contrast, malonyl-CoA synthesized by mitochondrial ACC2 acts mainly as an inhibitor of β-oxidation (17). We cannot clarify at present which ACC contributes to serum MA concentration but both ACCs regulate de novo lipogenesis in a coordinated and complementary manner (18).

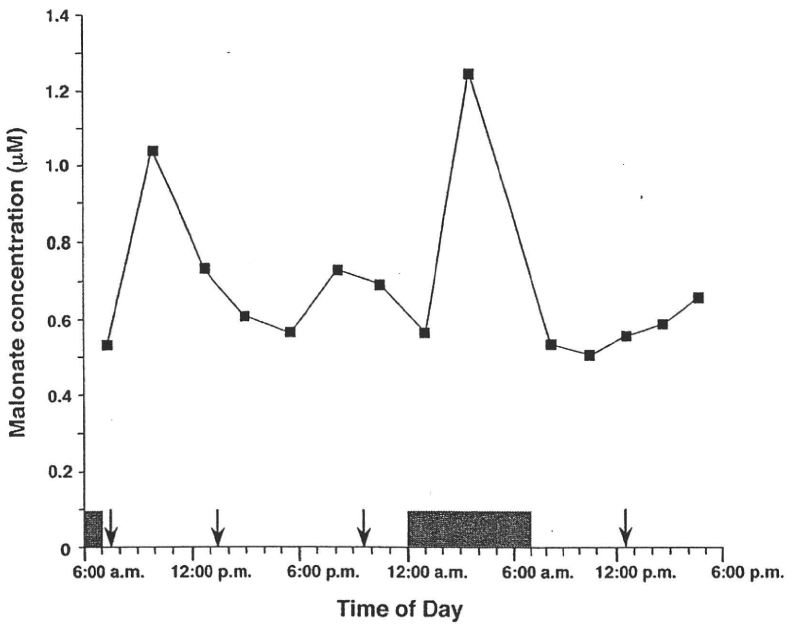

Fig. 5. The circadian rhythm of the serum levels of MA in a healthy volunteer. Blood samples were taken every 2–3 h. On the first day the volunteer consumed a normal hospital diet at 7:30 AM, 1:30 PM, and 9:30 PM (indicated by the arrows), and slept from 12:00 AM to 7:00 AM (indicated by the shaded box). On the second day the volunteer did not eat breakfast but consumed a normal hospital diet at 12:30 PM.

Under special conditions, however, other enzymes, MCD, and FAS can also be determinants of tissue malonyl-CoA levels and serum MA concentrations. For example, when MCD activity is reduced, such as with MCD deficiency, serum MA concentrations are elevated. Alternatively, when FAS is blocked by any drugs, such as C75 and cerulenin (2), MA concentrations increase in spite of reduced de novo FAS. Therefore, it is important to rule out the presence of such special conditions when we use serum MA as a biomarker for de novo FAS.

In summary, we developed a new method for the quantification of MA in human serum, which can be a good marker for de novo FAS. Derivatization of MA into DMP-MA allowed it to be quantified by LC-P-ESI-MS/MS with excellent sensitivity. Recovery and reproducibility experiments verified that this method provided highly reliable and reproducible analytical results.

The authors wish to thank the late Dr. Hiroshi Miyazaki for his helpful advice regarding mass spectrometry.

REFERENCES

1. McGarry, J. D., S. E. Mills, C. S. Long, and D. W. Foster. 1983. Observations on the affinity for carnitine, and malonyl-CoA sensitivity, of carnitine palmitoyltransferase I in animal and human tissues. Demonstration of the presence of malonyl-CoA in non-hepatic tissues of the rat. *Biochem. J.* **214:** 21–28.
2. Wolfgang, M. J., and M. D. Lane. 2006. The role of hypothalamic malonyl-CoA in energy homeostasis. *J. Biol. Chem.* **281:** 37265–37269.
3. Yoshida, T., A. Honda, H. Miyazaki, and Y. Matsuzaki. 2008. Determination of key intermediates in cholesterol and bile acid biosynthesis by stable isotope dilution mass spectrometry. *Anal. Chem. Insights.* **3:** 45–60.
4. Gao, J., L. Waber, M. J. Bennett, K. M. Gibson, and J. C. Cohen. 1999. Cloning and mutational analysis of human malonyl-coenzyme A decarboxylase. *J. Lipid Res.* **40:** 178–182.
5. Tanaka, K., D. G. Hine, A. West-Dull, and T. B. Lynn. 1980. Gas-chromatographic method of analysis for urinary organic acids. I. Retention indices of 155 metabolically important compounds. *Clin. Chem.* **26:** 1839–1846.
6. Tanaka, K., A. West-Dull, D. G. Hine, T. B. Lynn, and T. Lowe. 1980. Gas-chromatographic method of analysis for urinary organic acids. II. Description of the procedure, and its application to diagnosis of patients with organic acidurias. *Clin. Chem.* **26:** 1847–1853.
7. MacPhee, G. B., R. W. Logan, J. S. Mitchell, D. W. Howells, E. Tsotsis, and D. R. Thorburn. 1993. Malonyl coenzyme A decarboxylase deficiency. *Arch. Dis. Child.* **69:** 433–436.
8. Santer, R., R. Fingerhut, U. Lässker, P. J. Wightman, D. R. Fitzpatrick, B. Olgemöller, and A. A. Roscher. 2003. Tandem mass spectrometric determination of malonylcarnitine: diagnosis and neonatal screening of malonyl-CoA decarboxylase deficiency. *Clin. Chem.* **49:** 660–662.
9. Hirayama, T., A. Honda, Y. Matsuzaki, T. Miyazaki, T. Ikegami, M. Doy, G. Xu, M. Lea, and G. Salen. 2006. Hypercholesterolemia in rats with hepatomas: increased oxysterols accelerate efflux but do not inhibit biosynthesis of cholesterol. *Hepatology.* **44:** 602–611.
10. Shiina, I., R. Ibuka, and M. Kubota. 2002. A new condensation reaction for the synthesis of carboxylic esters from nearly equimolar amounts of carboxylic acids and alcohols using 2-methyl-6-nitrobenzoic anhydride. *Chem. Lett. (Jpn.).* **31:** 286–287.
11. Taguchi, G. 1986. Introduction to Quality Engineering—Designing Quality into Products and Process Asian Productivity Organization, Tokyo.
12. Honda, A., Y. Mizokami, Y. Matsuzaki, T. Ikegami, M. Doy, and H. Miyazaki. 2007. Highly sensitive assay of HMG-CoA reductase activity by LC-ESI-MS/MS. *J. Lipid Res.* **48:** 1212–1220.
13. Yamashita, K., S. Kobayashi, S. Tsukamoto, and M. Numazawa. 2007. Synthesis of pyridine-carboxylate derivatives of hydroxysteroids for liquid chromatography-electrospray ionization-mass spectrometry. *Steroids.* **72:** 50–59.
14. Schmedes, A., and I. Brandslund. 2006. Analysis of methylmalonic acid in plasma by liquid chromatography-tandem mass spectrometry. *Clin. Chem.* **52:** 754–757.
15. Hudgins, L. C., M. K. Hellerstein, C. E. Seidman, R. A. Neese, J. D. Tremaroli, and J. Hirsch. 2000. Relationship between carbohydrate-induced hypertriglyceridemia and fatty acid synthesis in lean and obese subjects. *J. Lipid Res.* **41:** 595–604.
16. Timlin, M. T., and E. J. Parks. 2005. Temporal pattern of de novo lipogenesis in the postprandial state in healthy men. *Am. J. Clin. Nutr.* **81:** 35–42.
17. Abu-Elheiga, L., W. R. Brinkley, L. Zhong, S. S. Chirala, G. Woldegiorgis, and S. J. Wakil. 2000. The subcellular localization of acetyl-CoA carboxylase 2. *Proc. Natl. Acad. Sci. USA.* **97:** 1444–1449.
18. Postic, C., and J. Girard. 2008. Contribution of *de novo* fatty acid synthesis to hepatic steatosis and insulin resistance: lessons from genetically engineered mice. *J. Clin. Invest.* **118:** 829–838.

新しい臨床検査

腫瘍マーカー

肝細胞癌の腫瘍マーカー

池上 正* 松崎靖司*

Key Words

AFP
PIVKA-II（DCP）
AFP-L3
肝癌診療ガイドライン

* 東京医科大学茨城医療センター
消化器内科

肝臓癌はわが国における癌死亡患者中第3位の頻度を占め，慢性ウイルス肝炎感染の高い罹患率とあいまって，消化器関連癌のなかでも臨床上大きな問題となってきた．近年HCVに対するインターフェロン療法の改良，さらにHBVに対する抗ウイルス薬の開発がすすみ，10年前に比較とするとウイルス肝炎そのもののコントロールは格段に進歩している．これらの抗ウイルス治療の進歩は今後肝癌患者の数を激減させるものと予想される．しかし，現時点で一般臨床の現場では肝癌の早期発見，治療はいまだ重要な課題の一つであることは異論のないところであろう．

わが国の肝癌診療ガイドライン（2005年）[1]に示された肝細胞癌サーベイランスのアルゴリズムのなかでは，B型慢性肝炎，C型慢性肝炎，肝硬変のいずれかが存在すれば肝細胞癌の高危険群，さらにB型肝硬変，C型肝硬変を超高危険群と設定している．ガイドラインではこれらの高リスク群に対して，画像検査，ならびに腫瘍マーカーの測定によって肝細胞癌をサーベイランスすることを推奨している（図1）．

本稿においては，現段階で肝細胞癌のマーカーとして用いられているものを概説し，実際的な使用方法について述べる．

alpha-Fetoprotein（AFP）

AFPは胎児期に肝および卵黄嚢（yolk sac）から産生される，分子量7万，590アミノ酸からなる糖タンパクである．妊娠12～15週ころ最も多く産生されるとされ，アミノ酸配列はアルブミンと約40%の相同性をもち，胎生期にアルブミンと類似した機能を果たしていると考えられている．1歳を過ぎると生体内ではほとんど産生されなくなるが，肝細胞の癌化などにより，蛋白産生調節も幼若化をきたすと，再び産生されるようになると考えられる．

日本肝癌研究会による第17回全国原発性肝癌追跡調査報告（2002～2003年の全国集計）[2]によれば，肝細胞癌16,766例中，AFP上昇（カットオフ値は15 ng/mL）を示した症例は10,075例，60%に至っている．肝細胞癌のほか，急性および慢性肝炎，肝硬変でも上昇がみられるため，とくに慢性ウイルス性肝炎患者においてAFP値をフォローするときは注意が必要である．青柳らの報告によると，20

0370-999X/09/¥100/頁/JCOPY

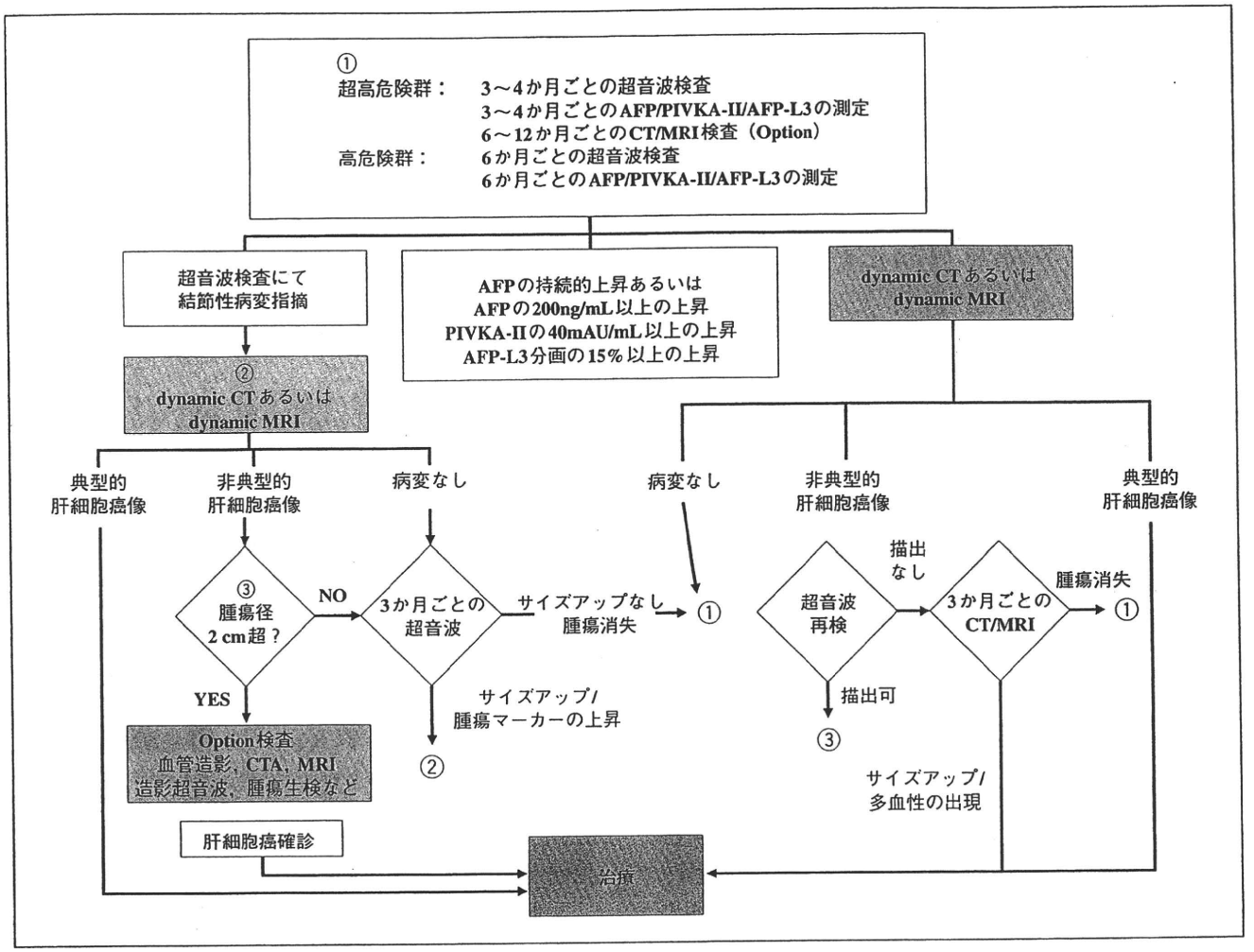

図1　肝癌診療ガイドラインによる，肝細胞癌サーベイランスアルゴリズム

ng/mLをカットオフ値としたとき，肝硬変，慢性肝炎症例の20%前後が陽性を示しており，肝細胞癌症例，良性肝疾患での平均値に有意な差は認めなかったとしている．このように，特異度の低さから，ワンポイントのAFP値から肝細胞癌と良性肝疾患を鑑別するのは困難であり，一般的には経時的な観察が必要であることが多い．すなわち，上昇したAFPが再び低下する場合には肝炎に伴う良性の変化であることが多く，また漸増する場合は肝細胞癌の存在を疑う．前述した肝癌診療ガイドラインにおいては，AFPの持続的上昇あるいは200 ng/mL以上の上昇を認めた場合，超音波，さらに造影CTもしくはMRIの撮像を推奨している．

AFP-L3

前述した良性肝疾患でのAFP陽性例という問題を解決すべく，青柳らが開発したのが肝細胞癌特異的なAFPの分画である[3]．彼らは，肝細胞癌由来AFPでは，良性肝疾患由来AFPに比較してレンズマメレクチンに親和性を有する画分の増加を認め，このAFPは二分岐複合型糖鎖の還元末端側のN-アセチルグルコサミンにα 1-6フコースが結合していることをみいだした（図1）[3]．現在このフコシル化AFP分画はL3分画として保険収載されている．前述した第17回全国原発性肝癌追跡調査報告[2]では，L3分画が測定された肝細胞癌6,321例中，感度以下であったものが35%を占めた．一方，カットオフ値を10%にすると全体の35%が，15%にすると30.7%が陽性で

あった．通常のAFP測定では，500 ng/mL以下の症例の中ではHCCと良性肝疾患のオーバーラップがきわめて多いが，これらの症例でL3分画を求めてみると，HCC症例が30±29％程度の割合だったのに対し，良性肝疾患では4±7％であり，AFP濃度では良悪性の鑑別が困難な症例においてAFP-L3の測定は有意義であると思われる．また，Tadaらは，切除された直径5 cm未満のHCC111例のうち，33例がAFP-L3陽性（カットオフ≧10%）であり，これらの腫瘍は病理学的な進行度が有意に高かった，としており[4]，本測定法の肝細胞癌の予後予知因子としての重要性を強調する報告も多い．

AFP高値にもかかわらず，画像検査にて肝細胞癌が同定できないとき，L3分画測定が有用な情報を与えてくれる可能性が高い．また，多くの検査会社では，L3分画測定時にAFPの総量も同時に報告してくれるため，AFPとL3分画を同時に測定する必要はない．前述の肝癌診療ガイドラインでは，AFP-L3のカットオフ値を15%と設定し，これ以上の場合は画像検査を行うことを推奨している．

PIVKA-II（DCP）

Protein induced by vitamin K absence or antagonist-II の略で，Des-gamma carboxy-prothorombin（DCP）ともよばれており，わが国で開発され，1989年以降保険適用となって以来AFPと並ぶ肝細胞癌の腫瘍マーカーとして普及してきた．通常肝臓で生成されるプロトロンビンは細胞内でプロペプチドとなり，gamma-carboxylationを受ける．Gamma-carboxylationはビタミンK依存性に活性化されるが，このcarboxylationが非効率的であると異常プロトロンビン（PIVKA-II）が産生される（図2）．

DCPは肝細胞癌に対する特異性が高いとされるが，閉塞性黄疸でビタミンKが欠乏している場合や，薬剤投与例（ワーファリン，セフェム系抗生物質の一部）で高値をきたすことがあり，注意を要する．また，アルコール性肝障害，肝硬変では軽度の上昇がしばしば認められる．

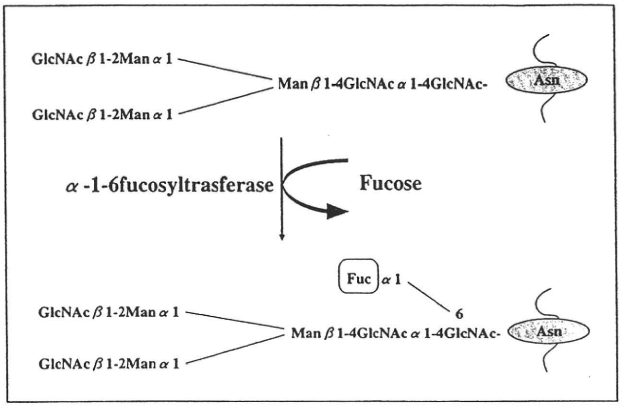

図2　AFPのフコシル化のシェーマ

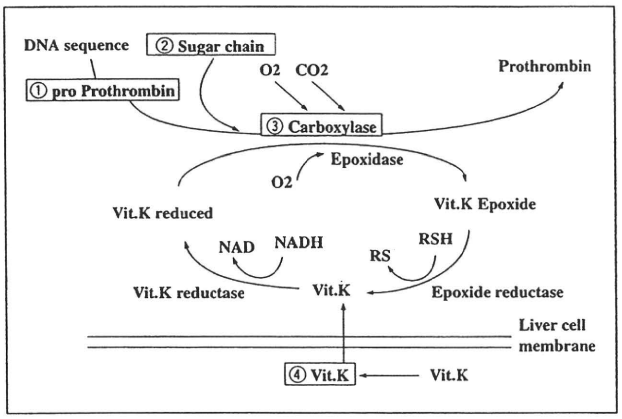

図3　プロトロンビン産生のシェーマ
肝細胞癌患者では明らかなビタミンK低下は認められておらず，PIVKA-II産生のメカニズムとして，①プロペプチドの異常，②糖鎖の異常，③カルボキシラーゼの異常，④ビタミンK取り込みの異常，などのメカニズムが考えられている．

第17回全国原発性肝癌追跡調査報告（2002～2003年の全国集計）[2]によれば，PIVKA-IIが測定された肝細胞癌14,209例中，PIVKA-IIが上昇（カットオフ値は40 mU/mL）を示した症例は8,376例，58.9％に至っている．AFPとPIVKA-IIの上昇が同時にみられない症例が多く，その意義はAFPと異なるとされる．門脈腫瘍塞栓を呈したHCC症例でPIVKA-II上昇例が多い[5]とされているが，最近発表された論文では門脈塞栓との関連は乏しいとする

ものもある[6]．また，トランスアミナーゼが比較的低値であり，血小板数が保たれている症例でPIVKA-II優勢HCCがAFP優勢HCCに比べて多い[6]，などの特徴が報告されている．また，別の報告ではPIVKA-IIが生命予後の判定に重要な鍵を握っていることが示されている[7]．諸外国でもこのマーカーの価値を評価するものも多いが[8]，2005年にアメリカ肝臓病学会が発表した肝細胞癌診断のガイドラインではまだ一般的なマーカーとして認知されるには至っていない．前述の肝癌診療ガイドラインでは，DCPのカットオフ値を40 mAU/mLと設定し，これ以上の場合は画像検査を行うことを推奨している．

各種腫瘍マーカーの使いかた

保険診療のなかでは肝細胞癌に対する腫瘍マーカー（AFP,DCP）の同時測定が2008年4月から認められるようになったことは，スクリーニングや治療後のフォローアップの精度上昇という観点からみても好ましいことであるといえる．したがって，現状では肝細胞癌の高リスクグループに属する患者に対して，AFPとDCPの同時測定を超高危険群では3～4か月に1回，高危険群では6か月に1回行うこと，またAFPが高値であるが画像診断上肝腫瘤が明らかでない症例に対してAFP-L3の測定を組み合わせることで，肝細胞癌の存在診断に重要な情報を得ることができる．しかしこれらの腫瘍マーカーが陰性の肝細胞癌が存在することもまた事実であり，腫瘍マーカーのみの測定で事足れりとすべきではない．前述のサーベイランスアルゴリズムにおいても，腫瘍マーカーの測定は補助的な位置づけとなっており，画像検査を積極的に組み合わせる必要がある．超音波検査や造影CT,MRIについては術者，あるいは施設間での精度にばらつきがあるため，したがって高危険群をフォローする際は信頼できる専門医，医療機関との連携が不可欠である．

文　献

1) 科学的根拠に基づいた肝癌診療ガイドライン作成に関する研究班：肝癌診療ガイドライン．東京：金原出版，2005
2) 日本肝癌研究会．第17回全国原発性肝癌追跡調査報告，2007
3) Aoyagi Y, Suzuki Y, Isemura M, et al.：The fucosylation index of alpha-fetoprotein and its usefulness in the early diagnosis of hepatocellular carcinoma. Cancer 61：769-774, 1988
4) Tada T, Kumada T, Toyoda H, et al.：Relationship between Lens culinaris agglutinin-reactive alpha-fetoprotein and pathologic features of hepatocellular carcinoma. Liver Int 25：848-853, 2005
5) Koike Y, Shiratori Y, Sato S, et al.：Des-gamma-carboxy prothrombin as a useful predisposing factor for the development of portal venous invasion in patients with hepatocellular carcinoma：a prospective analysis of 227 patients. Cancer 91：561-569, 2001
6) Yano Y, Yamashita F, Kuwaki K, et al.：Clinical features of hepatitis C virus-related hepatocellular carcinoma and their association with alpha-fetoprotein and protein induced by vitamin K absence or antagonist-II. Liver Int 26：789-795, 2006
7) Nagaoka S, Yatsuhashi H, Hamada H, et al.：The des-gamma-carboxy prothrombin index is a new prognostic indicator for hepatocellular carcinoma. Cancer 98：2671-2677, 2003
8) Marrero JA, Su GL, Wei W, et al.：Des-gamma carboxyprothrombin can differentiate hepatocellular carcinoma from nonmalignant chronic liver disease in american patients. Hepatology 37：1114-1121, 2003

著者連絡先

（〒300-0395）
茨城県稲敷郡阿見町中央3-20-1
東京医科大学茨城医療センター　消化器内科
池上　正

特集／感染症最前線

C型肝炎と肝癌
―肝炎から肝癌まで：とくに慢性C型肝炎治療の最近の知見―

東京医科大学 茨城医療センター 消化器内科 教授 松崎 靖司

はじめに

我が国の肝疾患患者数は，C型ウイルス肝炎のキャリアーの方が200万～300万人とも言われ，その中で肝硬変の患者は全国で40万～50万人前後と推計されている。肝硬変単独の死亡数は年間17,000人とされ，肝癌による死亡数は３万人とされている。2000年を境に肝癌死亡数は横ばいになりつつある。インターフェロン治療の普及の効果が多少現れてきているのだろうか。肝癌の原因の80％はC型肝炎ウイルス（HCV）に起因する。肝癌撲滅を目指すには慢性肝炎から肝硬変への移行を阻止することが大命題である。HCV抗体陽性者の自然経過は，HCV暴露から高率に慢性化し，20～30年後に肝硬変，そして肝細胞癌（HCC）発癌へと移行することが明らかとなってきている。

以上のような現況から，B型肝炎ウイルス（HBV），HCV，アルコールあるいはその他の発癌因子のHCC発生への関与の解明は急務となってきているといっても過言ではない。C型慢性肝炎から不幸にも肝硬変になった患者さんの場合は肝癌の早期発見をし，早期治療することが重要課題である。

本稿では，肝癌撲滅を目指し，その目的達成のために特にC型慢性肝炎から肝硬変への移行を阻止するための治療法，インターフェロン（IFN）療法，ウルソデオキシコール酸（UDCA）療法，プロテアーゼ阻害剤について最新の知見を概説する。

HCV抗体陽性慢性肝炎患者における治療法

I　インターフェロン療法

現在のC型慢性肝炎の治療はインターフェロン（IFN）が主流である。1991年にC型慢性肝炎に対してIFNが保険適応となり，2002年にリバビリンとの併用療法が保険適応となるまでは，全C型慢性肝炎患者のウイルス排除／陰性化（SVR）率は約30％であった。その後，2002～2004年まではリバビリン併用により効果も約45％に上がり，2006年現在は持続型IFN・リバビリン併用療法により，C型慢

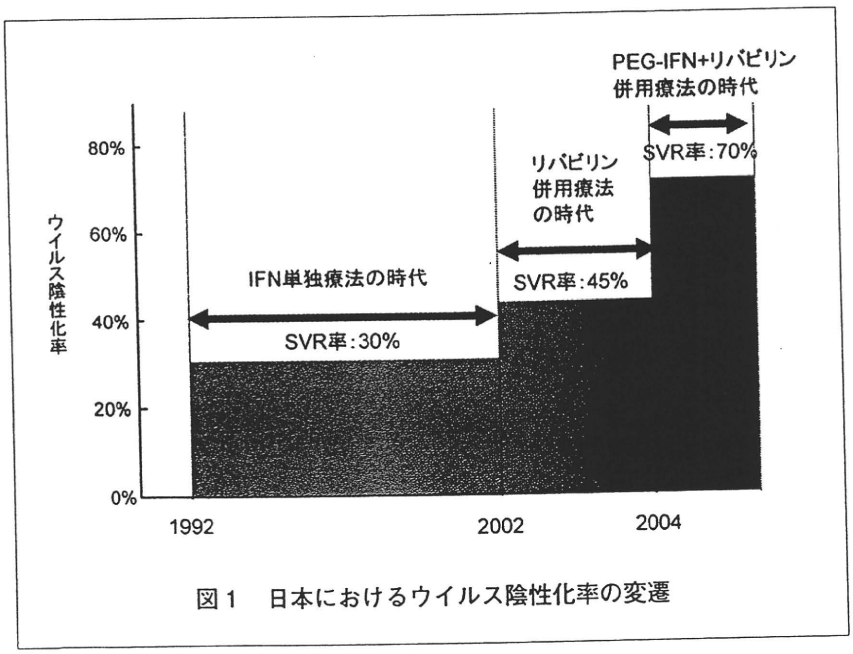

図１　日本におけるウイルス陰性化率の変遷